Experimental Study of Water Infiltration into a Partially Sealed Levee

Janssen, D.; Hommes, D. P.; Schmets, A. J.M.; Hofland, B.; Zwanenburg, C.; Dado, E.; Jonkman, S. N.

DOI
10.1061/JGGEFK.GTENG-12118

Publication date
2024

Document Version
Final published version

Published in
Journal of Geotechnical and Geoenvironmental Engineering

Citation (APA)
Janssen, D., Hommes, D. P., Schmets, A. J. M., Hofland, B., Zwanenburg, C., Dado, E., & Jonkman, S. N. (2024). Experimental Study of Water Infiltration into a Partially Sealed Levee. *Journal of Geotechnical and Geoenvironmental Engineering*, *151*(1), Article 04024139. https://doi.org/10.1061/JGGEFK.GTENG-12118

ASCE

Experimental Study of Water Infiltration into a Partially Sealed Levee

D. Janssen[1]; D. P. Hommes[2]; A. J. M. Schmets[3]; B. Hofland[4]; C. Zwanenburg[5]; E. Dado[6]; and S. N. Jonkman[7]

Abstract: During extreme high-water events, the phreatic water level in levees will rise over time due to infiltration of water. This can promote slope instability or internal erosion, and eventually lead to structural failure. A potential solution is the application of an impermeable seal, such as a geotextile, to the levee's outer slope to locally reduce the inflow of water. In this study, the spatiotemporal effect of a seal on the phreatic surface level is investigated experimentally, both at laboratory scale for a homogeneous sand levee, and at full-scale for a more realistic levee design. On the two-dimensional laboratory scale, it was found that application of a seal does not significantly change the steady-state phreatic level, as expected from a theoretical perspective. However, the time for the phreatic surface level to reach steady state after a sudden external water rise was found to increase 25% to 50% in the cases with a seal. Similar results were found for the full-scale three-dimensional experiments, which showed that details of the soil–structure interface significantly influenced the effectiveness of the impermeable seal, increasing the time to steady state between 12% and 25%. A simple numerical transient groundwater flow model confirms that the quality of the seal governs the response of the phreatic level. This model required the inclusion of an interface layer to properly model the imperfect soil–seal conditions. It is concluded that application of an impermeable seal to a levee before sudden water rise does not influence the new steady-state phreatic level. However, the seal slows down the infiltration process, especially for a case where the outer slope is damaged. **DOI: 10.1061/JGGEFK.GTENG-12118.**

Introduction

During extreme high-water events, a levee system will be subjected to increased hydraulic loads, which may trigger various failure paths (Van et al. 2022). These failure paths include both internal and external processes. Internal processes are caused by a rising phreatic surface level in the levee, whereas external processes are caused by, e.g., wave loads and lateral flow. The various failure processes can enhance each other, leading to failure of the levee, followed by an uninterrupted water flow through the levee breach into a low-lying area. Implementing an emergency measure means externally intervening in the damage process to locally improve the strength of a levee. Here, we focus on the effect of an emergency response intervention that intends to affect the development of the phreatic levels in a levee due to riverside infiltration, which may promote damage processes.

Historical attempts to decrease the water infiltration into a levee often included the application of geotextiles. In 1995, a levee along the River Rhine, near Ochten, Netherlands, which showed visual deformations of the levee body, was covered with geotextile to prevent levee failure (TAW 1995). The levee survived; however, the contribution of this emergency measure on the local resistance of the levee was not determined then. In case of damage of the outer levee slope, guidelines for emergency response to block the inflow of seepage water basically recommend the use of geotextiles surrounded by sandbags (Hofmann et al. 2006). These guidelines are based on best practice, but little is known about the increment in local resistance to water inflow that can be achieved by applying these measures.

Circumstances might be such that placement of a seal is preferred from the water side. This can be achieved by transporting a floating stiff structure over the water to the required location. The floating structure's bottom then holds a flexible sheet, which is able to adjust to the levee surface. Through partially submerging the structure at the site of interest, a seal at the levee's outer surface is established, kept in place by the anchored structure. This waterborne emergency method can be realized by using a military pontoon as the floating structure (Janssen et al. 2021). In this way, one can simultaneously locally raise a levee's crest and partly seal its outer surface. The phreatic level response of such seal is the subject under investigation in this study. Furthermore, the influence of the pressure that holds the seal in place will be neglected here.

Here, we consider a levee as a soil structure that allows infiltration of external water given an external water source at an elevated

[1]Ph.D. Student, Dept. of Hydraulic Structures and Flood Risk, Delft Univ. of Technology, Stevinweg 1, 2628 CN Delft, Netherlands; Netherlands Defence Academy, Het Nieuwe Diep 8, 1781 AC Den Helder, Netherlands (corresponding author). ORCID: https://orcid.org/0000-0002-3015-062X. Email: d.janssen@tudelft.nl

[2]Master's Student, Dept. of Hydraulic Structures and Flood Risk, Delft Univ. of Technology, Stevinweg 1, 2628 CN Delft, Netherlands. ORCID: https://orcid.org/0009-0006-6789-6472

[3]Assistant Professor, Dept. of Military Engineering, Netherlands Defence Academy, Het Nieuwe Diep 8, 1781 AC Den Helder, Netherlands. ORCID: https://orcid.org/0000-0003-2359-4633. Email: ajm.schmets@mindef.nl

[4]Associate Professor, Dept. of Hydraulic Structures and Flood Risk, Delft Univ. of Technology, Stevinweg 1, 2628 CN Delft, Netherlands. ORCID: https://orcid.org/0000-0003-1643-6469. Email: b.hofland@tudelft.nl

[5]Assistant Professor, Dept. of Geo-Engineering, Delft Univ. of Technology, Stevinweg 1, 2628 CN Delft, Netherlands. Email: cor.zwanenburg@deltares.nl

[6]Associate Professor, Dept. of Military Engineering, Netherlands Defence Academy, Het Nieuwe Diep 8, 1781 AC Den Helder, Netherlands. Email: e.dado@mindef.nl

[7]Professor, Dept. of Hydraulic Structures and Flood Risk, Delft Univ. of Technology, Stevinweg 1, 2628 CN Delft, Netherlands. Email: s.n.jonkman@tudelft.nl

Note. This manuscript was submitted on July 16, 2023; approved on July 11, 2024; published online on October 23, 2024. Discussion period open until March 23, 2025; separate discussions must be submitted for individual papers. This paper is part of the ***Journal of Geotechnical and Geoenvironmental Engineering***, © ASCE, ISSN 1090-0241.

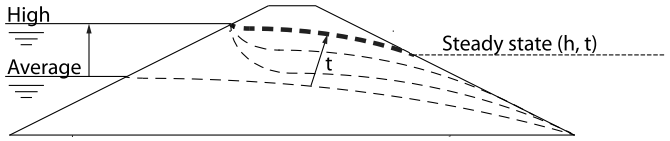

Fig. 1. Development of the phreatic surface level in space (h) and time (t) through a levee after a sudden increase of the outer water level from average to extreme (high) conditions.

hydraulic head levels. For the case of a high-water wave in a river, this pore water will flow through the structure is caused by the hydraulic pressure difference between the river and the landside of the levee. The same effect may also be caused by precipitation and evaporation (CIRIA 2013). Related to water flow within a levee during extreme water events, two fundamental time scales can be identified: the duration of the flood wave, and the time required for the phreatic surface to adjust to a new steady-state situation (Beber et al. 2023; Vahedifard et al. 2020). In the case considered here, schematized in Fig. 1, the water in the river rises from average to elevated or high levels. Subsequently, the phreatic surface level in the levee will adjust until a stationary state has been reached. This new steady-state pressure head h on a specific location in the levee is reached at time t.

Levee failure mechanisms typically triggered by increased phreatic surface levels are slope instability and internal erosion (Schiereck 1998). Firstly, an increased phreatic surface leads to increased local water pressures and decreases the effective stress of the soil. Hence, the shear strength reduces, which ultimately leads to mobilizing of one or several consecutive slip planes, causing structural failure of the levee by slope instability (Van et al. 2022). Secondly, an increase of the phreatic level will also be accompanied by higher flow gradients in the levee, increasing the probability of internal erosion processes (Rijkswaterstaat 2019).

In this study, a heterogeneous levee is assumed to consist of a permeable core covered with a clay layer; this is assumed to be a Dutch standard levee immediately after construction (Rijkswaterstaat 2019). Local damage to the cover layer will reduce the resistance of the soil mass to water infiltration. The inflowing water will distribute itself in the three dimensions that make up the levee. The surface damage can have many physical causes, such as bad maintenance of the grass cover or impact damage by fallen trees. In recent years, the issue of burrowing animals in levees has become an important issue in the Netherlands (Van Den Berg and Koelewijn 2023), for example beaver dens that penetrate deep into the core of a levee (Žilys et al. 2009).

Here, we start from a prior observation that geotextiles have been applied to seal the outer slope of levees during high-water crises. This practice is experience-based; a more fundamental understanding of the underlying mechanism of the positive effect of a seal on the survival rate of levees during high-water crises is still needed. Obviously, placement of a seal will locally decrease the inflow rate of water, which consequently would measurably influence the spatiotemporal behavior of the phreatic level, at least when the system is considered purely two-dimensional. The change of phreatic level can then be related to the observed increase in failure resistance of a levee. Therefore, this study aims to research the phreatic surface's response to the placement of a seal at the outer slope of a levee.

A series of experiments has been designed to find out whether placement of a seal has a measurable and predictable influence on the phreatic surface. First, laboratory-scale experiments were conducted. These laboratory experiments can be considered to represent an almost two-dimensional case, i.e., the condition of an infinitely wide seal. Experiments intended to capture the phreatic response by measuring the pressure head throughout the levee as a function of location and time. These experiments were then repeated for field conditions at the real scale, which obviously would capture the three-dimensional effect of the seal if it were present. A final step toward actual but unfavorable emergency conditions was achieved by artificially introduced damage to the seal-covered outer slope and establishing the phreatic surface also for this scenario.

The laboratory experiments have been conducted on a homogeneous levee in the TU Delft Hydraulic Engineering Laboratory, and three-dimensional field experiments took place on a heterogeneous levee in the TU Delft test facility, Flood Proof Holland. The experimental scenarios can also be studied by numerical simulations. Comparison of experiment and simulation should allow to show whether a two-dimensional (2D) model already captures the essential features of the full-scale experiment. In a similar way, the quality of the seal could be obtained by comparing the temporal development of the phreatic line.

In conclusion, this research studies the effect of an impermeable seal placed at the outer slope of a levee. The anticipated effect of interest here is the change of the phreatic surface in space and time. This paper is further organized as follows. First, the conceptual framework of the spatiotemporal behavior of the phreatic surface in a levee, and how this framework changes when the outer slope is sealed in both ideal and nonideal circumstances, is presented. Then, the design and results of laboratory-scale experiments and the three-dimensional real-scale experiments are presented. Finally, comparison of the experimental results and numerical simulation contributes to better understanding of the mechanisms that lead to decreased likelihood of failure for sealed levees.

Conceptual Framework

Here, we introduce two conceptual frameworks that describe the effect of a seal on the spatiotemporal development of the phreatic surface level in a levee. The first framework holds for idealized conditions, assuming a perfect connection between the levee surface and the seal. The second framework includes an interface layer, which allows inclusion of nonidealized conditions (such as the irregularities of the levee surface and stiffness of the seal), aiming to be able to model realistic practical applications. Both cases assume idealized two-dimensional conditions.

Case of Perfect Connection

In idealized conditions, the connection between the seal and the soil is assumed to be perfect, without any voids. The length of the impermeable seal is considered a variable, which is expressed as a coverage ratio C [Eq. (1)]. The length of the seal, L_p, is the length of the seal from the outer water level to the lowest part of the seal. The length of the uncovered slope below water surface, L_w, is the length from the lowest part of the seal to the toe of the outer slope of the levee (Fig. 2)

$$C = \frac{L_p}{L_w + L_p} \times 100\% \tag{1}$$

If the outer levee slope is sealed to limit the inflow of water, the development of the phreatic surface level through a levee in space and time will adjust according to the new boundary conditions (Fig. 2). The length of the flow path will increase, caused by the presence of the seal. However, the total pressure head difference between the boundary conditions remains the same. This leads to a

J. Geotech. Geoenviron. Eng., 2025, 151(1): 04024139

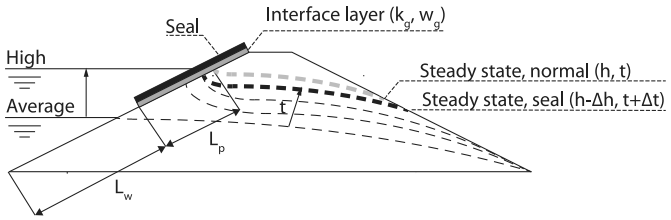

Fig. 2. Development of the phreatic surface level in space and time through a levee after an increase of the water level from average to extreme (high) conditions when applying an impermeable seal on the outer levee slope. Here, Δh = difference in phreatic surface level, Δt the difference in time to reach these conditions, as compared with the situation without a seal, k_g = resistance of the interface layer, and w_g = width of an interface layer. These values represent a nonidealized surface–seal connection.

reduced gradient of the flow and herewith a lower Darcy velocity (q). Thus the time to reach steady state (Δt) will increase compared with the case without a seal. Next to that, a reduction in steady-state phreatic water level (Δh) compared with the undisturbed case is expected.

Case of Imperfect Connection of Surface–Seal Interface Layer

The boundary conditions in the real world will not be perfect. The levee surface will, in practice never be entirely smooth, and the seal will not be able to completely adjust itself to these irregularities. The occurring surface–seal distances will allow water to flow underneath the seal. This water will be able to seep into the levee, reducing the effectiveness of the seal. This practical limitation requires the need for an extra interface layer in the conceptual model (Fig. 2). Two parameters are introduced to take account for these irregularities, the thickness (w_g) and the hydraulic conductivity of the new interface layer (k_g). The thickness w_g does essentially originate from irregularities of the outer slope of the levee. The hydraulic conductivity of the interface layer k_g represents the resistance of the infiltrating water flow in the interface layer, caused by the fraction of seal in contact with the levee its surface.

Lab-Scale Experiments

Experimental Setup for Lab Experiments

Experiments were conducted in a flume in the TU Delft Hydraulic Engineering Laboratory. These experiments aimed to determine the effect of a seal on the phreatic surface level through a model levee in space and time. A homogeneous sand levee with a width along the levee axis of 0.77 m and a height of 0.8 m was constructed in the sedimentation flume of the laboratory. The crest width of levee was set to 0.2 m, the gradient of the outer slope to 1:2, and the gradient of the inner slope to 1:3. This test setup is shown in Fig. 3. The inner slope of the levee was covered by a water-permeable geotextile, then covered by a gravel layer to avoid internal erosion, the movement of the grains on the inner slope caused by the exit gradient of the flow (Fig. 4). The levee was constructed by applying subsequently multiple layers of sand, each of approximately 5-cm thickness. After a layer was placed, it was compacted using the weight of a human-operated masonry trowel.

The levee was built out of standard silver sand. Several soil parameters were determined in the laboratory and are given in Table 1. The saturated permeability, k_{sat}, of the sand was determined with a falling head test. A HYPROP (UMS, Munich, Germany) experiment (Schindler 1980) was conducted to determine the soil water characteristic curves (SWCC) and the saturated volumetric water content, VWC_{sat}. The experiments to determine soil parameters were conducted with the same sand, but did not represent in situ soil samples, thus the sand may possess a different density in the experiment.

The local pressure head near the bottom was measured using electronic pressure sensors [Honeywell (Charlotte, North Carolina), 24PC] that were installed in standpipes in the cross section of the levee. Two rows of eight PVC standpipes were glued to the bottom of the flume. The center-to-center (ctc) distance of the standpipes in the direction parallel to the levee's crest was 0.35 m; the ctc distance in longitudinal direction was 0.29 m. The outer diameter of the PVC standpipes was 0.05 m. Water was able to flow into the standpipe through a water inlet, which was located between 0.04 and 0.08 m from the flume bottom. The pressure sensor automatically corrected for the atmospheric pressure by using a Wheatstone bridge. The output of the sensor was a voltage, which could be transformed into a water pressure using a calibration factor. The sampling interval of the sensors was set to 60 s.

Seepage water that flowed through the levee was collected in a seepage box, at the landward toe of the levee. The water level in the

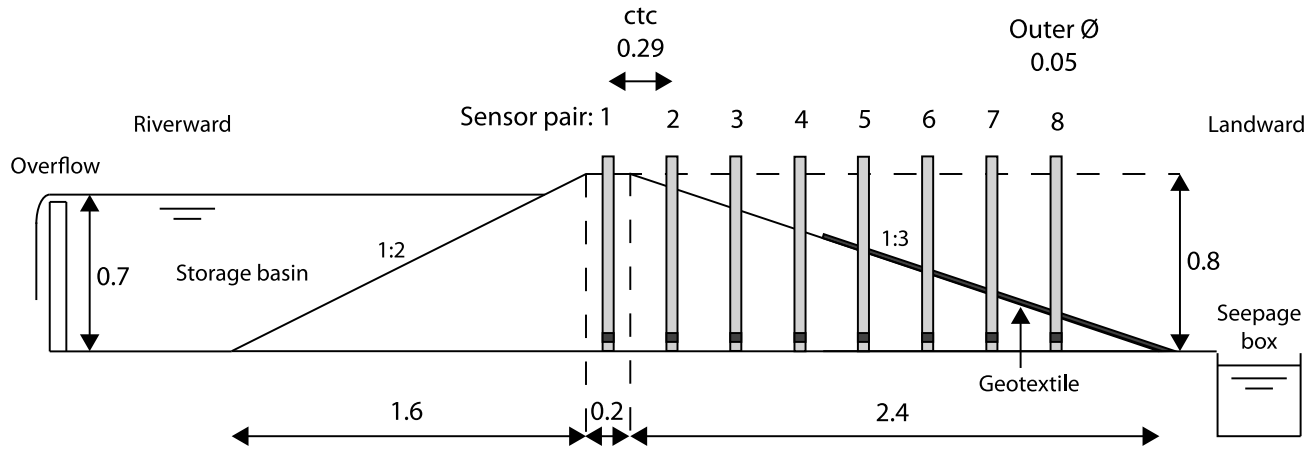

Fig. 3. Dimensions of test levee, sensor rows, and various important parameters (dimensions in meters).

J. Geotech. Geoenviron. Eng., 2025, 151(1): 04024139

(a) (b)

Fig. 4. (a) Landward; and (b) riverside view of the experimental setup for LT-4.

Table 1. Soil parameters silver sand from which the model levee has been constructed

Parameter	Value	Unit
d_{50}	0.4	mm
k_{sat}	5.12×10^{-3}	m/min
VWC_{sat}	0.347	—

box was measured using a Temposonics (Lüdenscheid, Germany) G-Series GH rod location sensor. The measurement interval of the rod was set to 60 s. The leakage discharge through the model levee was determined by determination of the fill rate of the box, correcting for its irregular shape.

The main goal of the experiments was to determine the effect of an impermeable seal on the phreatic surface level through a levee in space and time after a sudden increase of the outer water level. The seal consisted of an impermeable steel stiff plate (1.44-m length, 0.77-m width, and 8-mm thickness), covering the wetted outer slope of the levee (Fig. 4). To prevent water to enter the levee through the area between the plate and the glass sidewalls of the flume, this slit was closed with impermeable tape.

In total, four experiments were conducted, of which two experiments served as a repeated for the reference case without the application of a seal. The other two experiments were conducted with a near total coverage of the outer slope. The latter two experiments differed in the presence of a toe sealing the inlet at the bottom of the outer slope. This toe structure consisted of an extra layer of sand up to the lower edge of the seal plate. It is shown in Fig. 4(b). The reason for applying this toe was the openings that were observed between the plate and the sand body. These were caused by the stiffness of the plate and the irregularities of the outer slope, allowing water to flow underneath the plate. The maximum observed opening was approximately equal to the thickness of the plate (8 mm). The toe had a width of 10 cm and a height of 5 cm. The lab-scale experiments performed for the model levee with and without a steel seal cover at the outer slope of the model level are summarized in Table 2.

Table 2. Scaled lab experiments on phreatic response to sudden rise of water level

Test number	Coverage (%)	Note	Fill time (min)	Q_{steady} (L/s)	
				Sensor	Per m[1]
LT-1	0	Reference	44	0.026	0.034
LT-2	0	Reference	50	0.026	0.034
LT-3	99	—	42	0.026	0.034
LT-4	99	Riverward toe	41	0.022	0.026

Before the start of the experiment, the pressure sensors were turned on for at least 1 h to determine the initial conditions of the sensors. After this, water was allowed to enter the storage basin (Fig. 3) through a hose. The maximum water level was 0.7 m, which was enforced using an overflow structure at the end of the storage basin. During the experiments, a continuous inflow of water in the basin was maintained to keep a constant water level in the storage basin. The time needed to fill the storage basin, the fill time, is given in Table 2.

The output voltages of the pressure sensors were monitored during the experiment. When these voltages exhibited no increase in value at 10^{-3} digits for least 1 h, one could assume that the phreatic surface level in the levee had reached steady-state conditions. When these conditions were achieved, water was removed from the basin, and the pore water release process from the levee was measured in a similar way as during filling. A new experiment started if the water level, as measured by the pressure sensor, had equilibrated at the initial measured value. One experiment was performed per day.

Lab-Scale Measurement Results

The main results of the experiments are summarized in Table 3. It shows the time required to reach the steady state, t_{steady}, for each experiment together with the corresponding steady-state water level h_{steady}, for each location, in each pressure sensor. At $t = 0$, water starts to enter the basin. The time to steady state is the time required

Table 3. Main results laboratory experiments

Sensor pair	t_{steady} (min)				h_{steady} (m)			
	LT-1	LT-2	LT-3	LT-4	LT-1	LT-2	LT-3	LT-4
1	83	87	119	147	0.48	0.48	0.49	0.50
2	84	89	93	134	0.44	0.44	0.47	0.41
3	90	101	126	165	0.41	0.40	0.37	0.36
4	84	88	91	135	0.37	0.38	0.32	0.34
5	80	85	82	119	0.32	0.32	0.31	0.31
6	77	80	78	113	0.26	0.26	0.26	0.25
7	72	77	75	105	0.17	0.17	0.18	0.17
8	67	72	88	—	0.10	0.10	0.10	0.10
Mean	80	85	94	122		—		

Note: See Fig. 3 for sensor locations.

from opening the hose at the start of an experiment until the measured gradient ($\partial h/\partial t$) in a certain sensor has become smaller than 1×10^{-3} m/min. The steady-state time has been determined after the experiments, incorporating the sensor specific voltage to height calibration factor. Visual inspection of Fig. 5 shows that even for the worst-case scenario, this criterion provided an adequate estimate of the steady-state time. Allowing a smaller gradient would increase the time to steady state, whereas the increment in water level would be small. The parameter h_{steady} is the maximum measured value of the individual sensor.

The steady-state leakage discharge data through the model levee, Q_{steady}, is provided in Table 2. The sensor steady-state discharge is the discharge as measured by the sensor, and the per m^1 value is the steady-state discharge corrected for the flume width. The steady-state leakage discharge was determined by measuring the water level in the discharge box over time.

Fig. 5 shows the measured phreatic water level for Sensor pairs 1, 3, 5, and 7 over time for the different tests (Table 2). The presented data are the data measured by the right sensor in the sensor row, as seen from the crest. For Sensor pairs 3 and 4, the measurements of the left sensor were used, caused a defect in the right sensor. Fig. 6 shows the spatial pattern of the phreatic surface level through the levee at different times at each sensor pair position, Fig. 6 is constructed from the data as presented in Fig. 5. The reported water levels are related to the initial conditions of the sensors.

The mean time required for the LT-1 and LT-2, the reference case, to reach steady-state conditions (t_{steady}) is the same order of magnitude of 80 to 85 min. The time to reach steady-state conditions for the LT-3 was about 40 min longer for the first three riverward sensor rows. However, this increase in time to steady state disappeared for the sensor rows closer to the landward toe of the levee, in line with expectations. In LT-4 (with seal and berm), the time required to reach steady-state conditions increased over the entire cross-sectional profile of the levee. Steady-state phreatic surface levels were found to be nearly equal for all the experiments. Only a slight lowering of the phreatic surface at Sensor pairs 3 and 4 may be present, although this difference is close to the measurement accuracy. This accuracy includes the accuracy of the sensors (±1 cm) and the measurement accuracy of the elevation of the sensors (±1 cm).

The presence of the toe at the bottom of the levee in LT-4 clearly showed a large influence on the development hydraulic head in the levee. Roughly up to 100 min, the phreatic level was significantly lower than in the case without toe and the reference case. This corresponds to an increase in time of 25% to 50% relative to the scenario without toe and the reference scenario, respectively, to reach the steady-state phreatic level.

Real-Scale Field Experiments

Experimental Setup of Field Experiments

To gain insight in the effects of an impermeable seal on the development of the phreatic surface level through a levee with a clay cover in space and time, experiments were prepared at the TU Delft test facility, Flood Proof Holland. These experiments aimed to

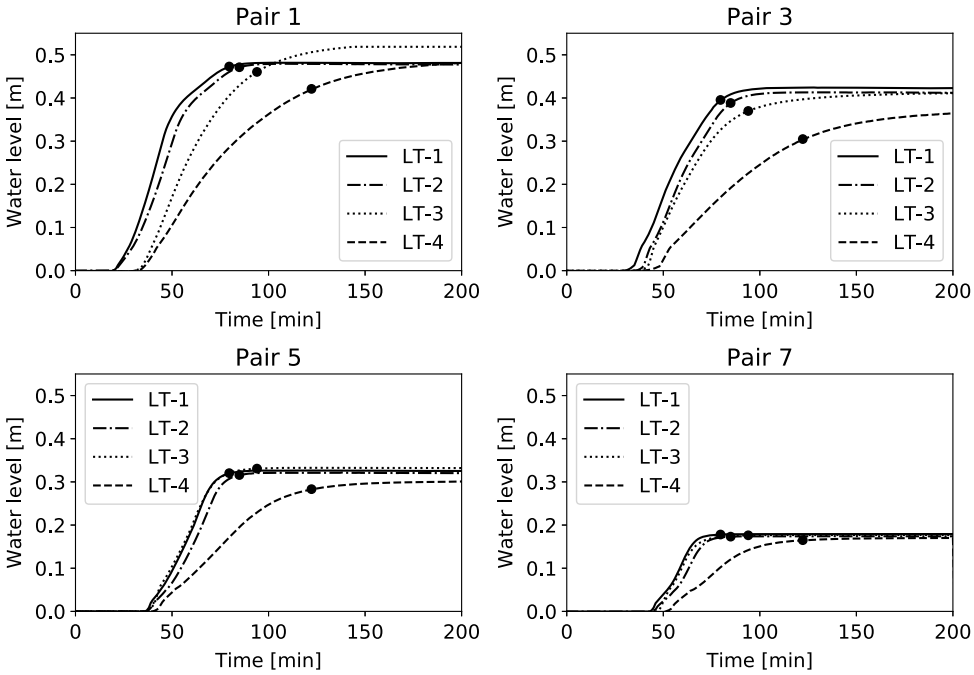

Fig. 5. Water level over time for Sensor pairs 1, 3, 5, and 7 in the model levee of the lab experiment. Solid dots represent steady-state time.

J. Geotech. Geoenviron. Eng., 2025, 151(1): 04024139

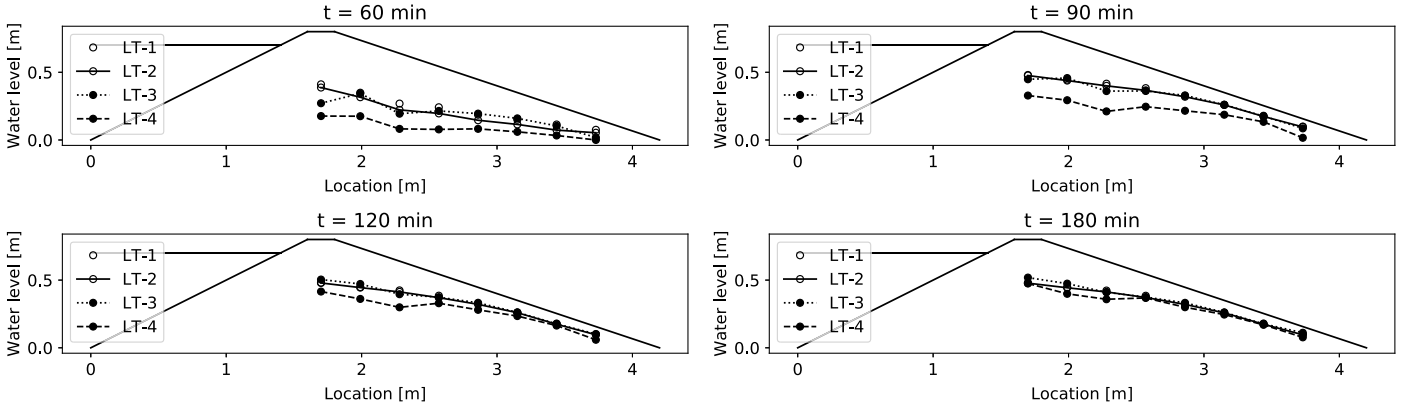

Fig. 6. Measured phreatic levels in the model levee at several times after riverside water level rise.

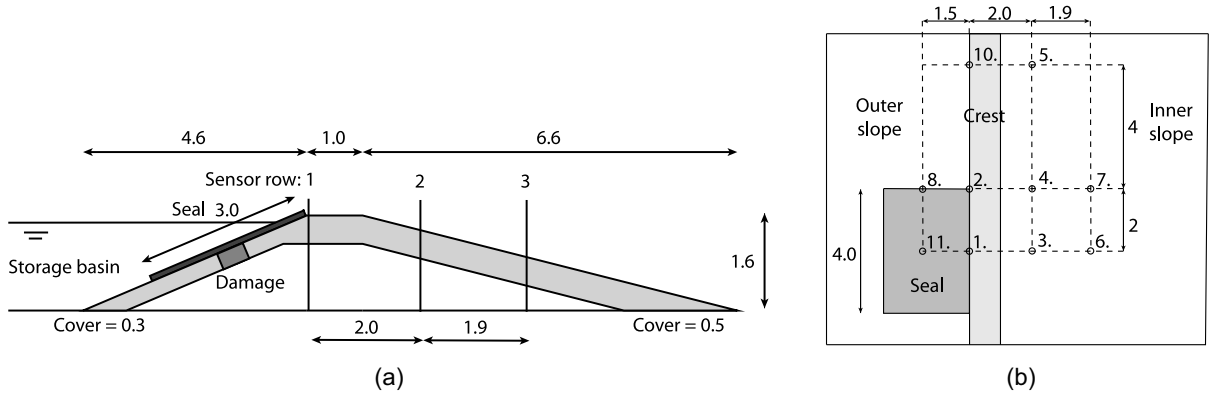

Fig. 7. (a) Cross section of the experimental setup at Flood Proof Holland, where damage is $0.5 \times 0.5 \times 0.3$ m and seal is 3.0×4.0 m (dimensions in meters); and (b) top view of experimental setup Flood Proof Holland, indicating the numbers and corresponding location of the applied sensors.

measure the development of the phreatic surface over time in a real heterogeneous levee. The levee consisted of a sand core ($k = 2.8 \times 10^{-3}$ m/min), covered by a clay layer ($k = 1.3 \times 10^{-4}$ m/min) overgrown by grass. The clay had a thickness of 0.3 m on the outer slope and 0.5 m on the inner slope of the levee. The levee had a height of 1.6 m and a crest width of 1.0 m. The 1:2.9 outer slope had a length of 4.6 m in horizontal direction and the 1:4.1 inner slope a length of 6.6 m. The experimental setup is shown in Fig. 7.

The goal of the experiments was to measure the response of the phreatic level for various conditions of the outer slope of the levee. Therefore, conditions have been prepared with and without damage to the clay layer to test the difference in response of the phreatic level. Laboratory measurements have indicated that the most important parameter to reduce the inflow of groundwater were the soil–structure contact details. The damage was achieved by digging a square hole on the outer slope of the levee, with dimensions of 0.5×0.5 m and a depth of 0.3 m; this depth is equal to the thickness of the cohesive clay cover material of the levee (Fig. 8). Reaching the core material was confirmed through a visually observed change of soil color. The damage was located in the center of the cover seal, at the location of Sensor 11 in Fig. 7.

Six different experiments were conducted, with different cover materials for the levee and two different damage cases (Table 4). The development of the phreatic surface level over space and time without a cover was compared with the scenarios with the damage covered by a semistiff plate and a flexible sheet. The plate cover consisted of a structure that was slightly able to adjust itself to the irregularities of the outer slope; the plate was made of plywood and weighted by sandbags. The sheet cover consisted of a flexible plastic sheet weighted by sandbags, which was able to adjust it shape to the irregularities of the levee surface. Both the plate and the sheet were 4 m wide in the direction of the crest and 3 m long perpendicular to the crest.

Within the levee, three rows of standpipes were placed (Fig. 7), which contained small holes to measure the phreatic surface level in the levee. The first row of three sensors was located at the center of the impermeable structure. The second row of three sensors was placed at the end of the structure, and the third row of two sensors was placed a few meters from the structure. In each standpipe, a Tasseron (Nootdorp, Netherlands) pressure sensor (6-m range) was placed, the measurement interval of the sensors was set to 15 min. The location of the sensors are represented by the dots. Filling of the approximately 150-m^3 basin took 45 min. A more detailed description of the test setup has been given by Hommes (2022).

Real-Scale Measurement Results

The time to steady state is, as previously, defined as the time to the state when the hydraulic gradient at the locations of the individual sensors, for the various test cases becomes smaller than 1×10^{-3} m/min . The steady-state values, t_s, for Sensors 1, 3, and 6,

J. Geotech. Geoenviron. Eng., 2025, 151(1): 04024139

(a)

(b)

(c)

Fig. 8. (a) Reference case with damage; (b) plate; and (c) sheet at Flood Proof Holland.

located along the centerline axis of the seal, in the direction perpendicular to the levee crest (Fig. 7), together with the average time to steady state for the three sensors can be found in Table 4. The time to reach steady-state conditions was found to increase for the undamaged Tests FT-3 and FT-5 compared with FT-1. The same trend was observed when comparing the tests with damage, FT-4 and FT-6, with FT-2. The observed increase in time to steady state was larger for the tests including a sheet compared with the tests with the plate.

In Fig. 9, the water level in the standpipes located at the center of the seal over time is plotted for the reference case (FT-1), the plate case (FT-3), and the sheet case (FT-5), all without damage to the outer slope of the levee. Comparing the reference case with the plate case (FT-1 and FT-3), it can be observed that the fill curves of both tests did not show any spatiotemporal differences in the filling behavior. When comparing the reference case with the sheet

Table 4. Real-scale experiments performed to measure the influence of a seal on the phreatic surface level in space and time

Test number	Seal	Damage	$t_{s,1}$ (h)	$t_{s,3}$ (h)	$t_{s,6}$ (h)	$t_{s,\text{mean}}$ (h)
FT-1	No	No	3.25	6.25	5.75	5.08
FT-2	No	Yes	3.25	6.00	5.75	5.00
FT-3	Plate	No	3.25	6.00	6.75	5.33
FT-4	Plate	Yes	3.25	6.50	6.00	5.25
FT-5	Sheet	No	3.25	6.75	7.00	5.67
FT-6	Sheet	Yes	5.25	6.75	6.00	6.00

Note: $t_{s,n}$ = steady-state time of a sensor (Fig. 7); and $t_{s,\text{mean}}$ = mean value of the three sensors shown.

case (FT-1 and FT-5), a difference in the fill curve can be observed: the curve for the undamaged sheet case showed an increment in time to reach steady-state conditions. This observed effect of the seal was larger near the crest (Sensor 1), whereas the effect of the seal closer to the inner toe of the levee was almost negligible (Sensor 6).

The development water level in the standpipes located in the center of the seal over time for the cases with damage to the outer slope of the levee, for the reference case (FT-2), the plate case (FT-4), and the sheet case (FT-6) is shown in Fig. 10. The same trends were observed as the cases without damage to the outer slope. The effect of a plate (FT-4), on the development of the phreatic surface was still minimal compared with the reference case (FT-2); however, the effect was more present compared with the cases without damage to the outer slope. The effect of a sheet on the fill curve with damage to the outer slope appeared to be more present when comparing it with the undamaged case, especially for Sensors 3 and 6.

These larger scale experiments on a heterogeneous levee confirm the effect of the soil–structure interface on the spatiotemporal behavior of the phreatic surface. The effect of the stiff plate was found to be negligible, but the flexible sheet clearly changed the behavior of the phreatic surface underneath it. The experimental data show that the reduction in phreatic surface level over time is only temporal. The effect of the seal was found to be larger for the case with damage to the clay layer on the outer slope of the levee.

Three-Dimensional Effects in Field Tests

Until now, the problem has been treated as purely two-dimensional, although in reality, the problem is completely three-dimensional. Fig. 11 shows a top view of the field tests performed in Flood Proof Holland 2 h after the start of the experiments. The dots in the figure represent the location of the standpipes. Fig. 11(a) shows the difference in measured water level between FT-1 and FT-5, the reference and the sheet tests for the undamaged outer slope. Fig. 11(b) shows the difference in measured water level between FT-2 and FT-6, the reference and the sheet test for the damaged outer slope. Both figures were obtained by multiquadratic interpolation of the measured values of the standpipes in the inner slope of the levee. Then, the interpolated values were mirrored along the center of the setup (lateral symmetry of the phreatic pattern was assumed).

Fig. 11 shows that the difference in phreatic surface level after 2 h with and without a seal was larger close to the crest than closer to the toe, which is in line with the two-dimensional representation of the results in Fig. 9 and Fig. 10. Furthermore, it can be observed that the influence of the seal in the y-dimension was larger with outer slope damage compared with the situation without damage. The effect of the dimensions of the seal in the y-direction in relation to the influence area of the seal is unknown.

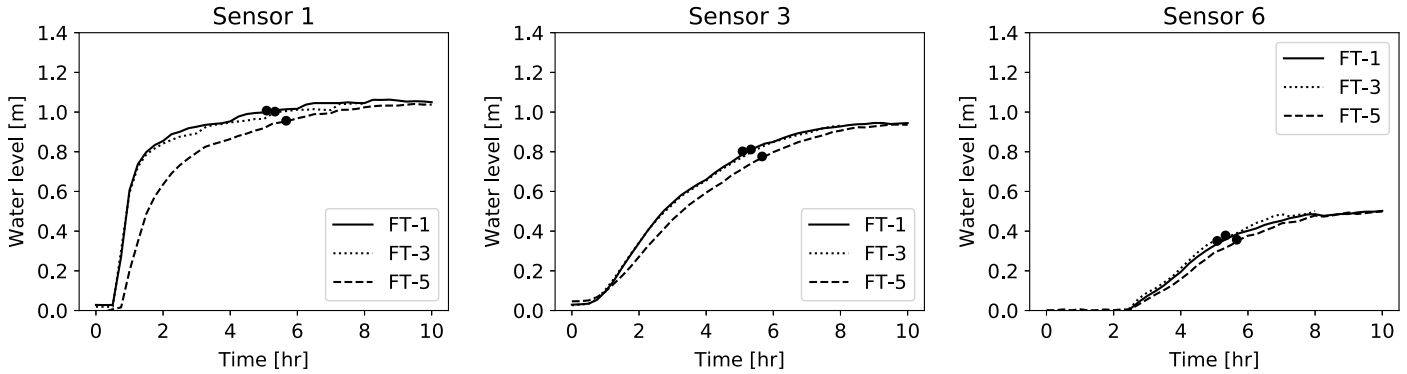

Fig. 9. Full-scale field trial results showing the results of FT-1 (no damage no seal), FT-3 (no damage with plate), and FT-5 (no damage with sheet).

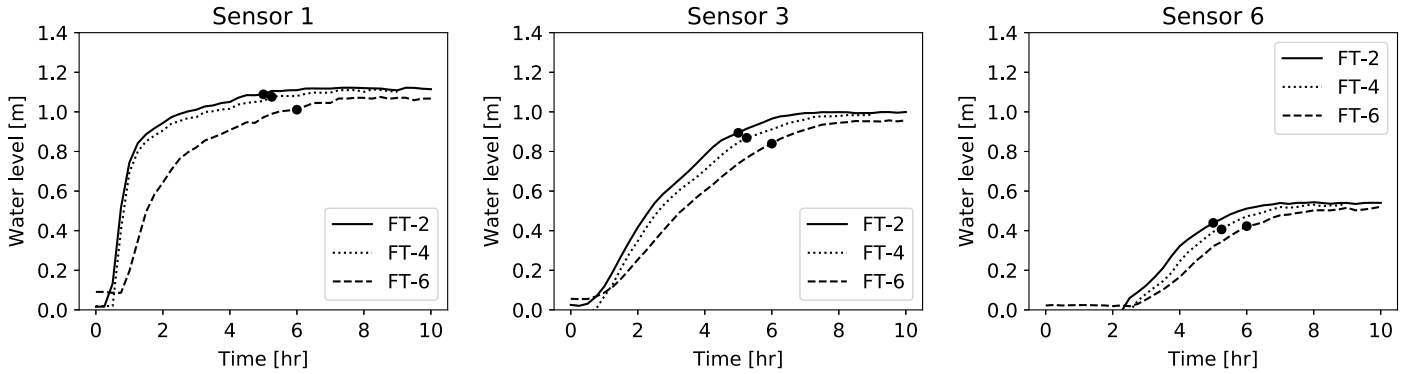

Fig. 10. Full-scale field trial results showing the results of FT-2 (damage no seal), FT-4 (damage with plate), and FT-6 (damage with sheet).

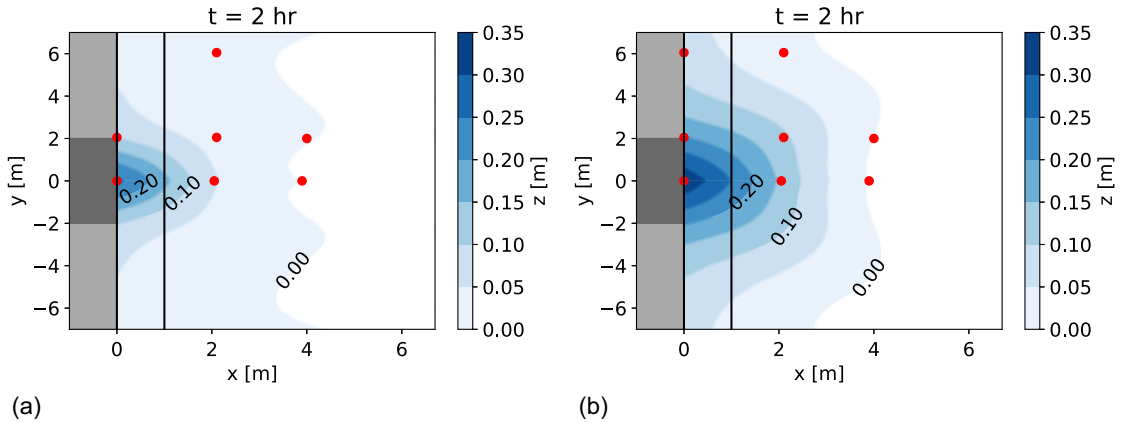

Fig. 11. Top view of the test setup and difference in phreatic surface over time between experiments: (a) FT-1 minus FT-5; and (b) FT-2 minus FT-6. Dots indicate the location of the standpipes. The region $-1 < x < 0$ represents the outer slope, $0 < x < 1$ represents the crest, and $x > 1$ represents the inner slope. The emergency measure (seal) is located on the outer slope between $-2 < y < 2$ and $-2.8 < x < 0$.

Numerical Estimates to Capture Soil–Structure Interface

In this section, we introduce a simplified numerical model to capture the possibilities of using an interface layer to estimate the spatiotemporal development of the phreatic surface through a levee covered by a seal. This exhibition has only be performed on the homogeneous sand levee, which was tested in the laboratory. NS-1 models the LT-1 case, NS-3 models the LT-3 case, and NS-4 models the LT-4 case. First, the case with a perfect soil–structure interface layer was modeled, where after the interface layer was added. The application of numerical simulations for the field tests are part of the discussion.

Numerical Model of the Laboratory Case

The model was built using the transient groundwater flow module of PLAXIS Limit Equilibrium (version 21), which solves Darcy's equations for both saturated and unsaturated groundwater flow problems (Bentley Systems Team 2021). The laboratory geometry,

J. Geotech. Geoenviron. Eng., 2025, 151(1): 04024139

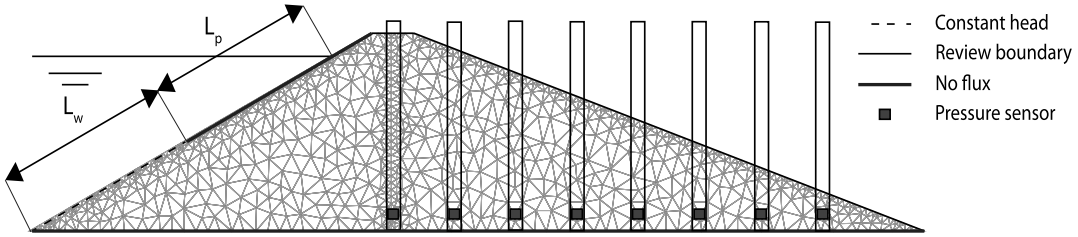

Fig. 12. Boundary conditions with closure and location pressure sensors in standpipes, including mesh for the numerical simulation of the laboratory experiments. Levee dimensions are the same as given in Fig. 3.

as presented in Fig. 3, was implemented in the model. The boundary conditions used for the model comprised a specific head boundary condition, where the head increased linearly to its maximum value of 0.7 m over a period of 50 min (Table 2). The impermeable bottom in the laboratory was modeled as a no-flux boundary. Because details of the outlet of the phreatic surface were not known, the inner slope was defined as a review or drain boundary condition. The review boundary determines the location where the pressure head is zero at the inner slope. Finally, the seal on the outer slope was defined as a no-flux boundary, where the ratio L_w and L_p was defined by the closure percentage (Fig. 12). The output value for the pressure sensors in the model correspond to the location of the water inlets of the standpipes as applied in the laboratory experiment.

The soil material is defined by the saturated permeability and the volumetric water content as defined in the laboratory (Table 1). The applied soil water characteristic curve was fitted using the Fredlund and Xing (1994) fit, which has been found to be a good representation of the SWCC (Rahimi et al. 2015). A triangular mesh was applied within the entire geometry, applying a minimum interior angle of 30°, a maximum length on region boundaries of 0.112 m, and a tolerance of 0.001 m, resulting in a mesh with 1,769 elements (Fig. 12). Increasing and decreasing the mesh density with a factor of 2 did not change the output results for the reference case.

Numerical Results: Steady-State Height

Fig. 13 shows the steady-state measured pressure heads in the laboratory for both LT-1 and LT-2 and the computed pressure height with the corresponding phreatic surface, NS-1, as obtained for the numerical model. The difference between simulated and measured pressure heads showed a decreasing trend toward the landward toe of the levee profile (ranging from 8 cm at Sensor pair 1 to 0 cm at Sensor pair 8). This difference in output value will not impact the results of the study because the main findings of the laboratory measurements are time differences and not pressure head differences in the steady state. These differences could either be caused by the effects in z-dimensions in the laboratory experiments or the measurement accuracy of the laboratory measurements. A method to deal with this difference could be the inclusion of a correction factor, which would only depend on the x-coordinate of the pressure sensor.

Fill Time

An important finding of the laboratory experiments was the additional time to reach steady-state conditions for a certain closure percentage after transient increase of riverside water levels. Because the soil was considered to be homogeneous, the shape of the phreatic surface and pressure head distribution for the steady state were not expected to vary with k. However, the time to reach steady-state conditions, t_{steady}, was expected to vary with k. The permeability of the soil was fitted to the time to steady state as measured in the laboratory experiments. Table 5 presents the results of the calibrated numerical model. Fig. 14 compares the measured and estimated fill rate in the pressure sensor over time for Sensor pairs 1, 3, 5, and 7. The lowest mean average error (MAE) was found for the model with a permeability factor k of 7.62×10^{-3} m/min.

Phreatic Surface Level in Ideal Conditions

To gain insight in the numerical prediction of steady-state level and the time required to reach this level, numerical runs were conducted for various closure percentages (Table 6), including the geometry (Fig. 3) and calibrated soil parameters from the heterogeneous laboratory tests ($k = 7.62 \times 10^{-3}$ m/min). The coverage percentage, as mentioned in the table, indicates the percentage of wetted outer slope covered by the impermeable seal [Eq. (1)]. There are two cases with a 50% coverage percentage. In the normal 50% case, the seal is covering the top half of the levee as in all other

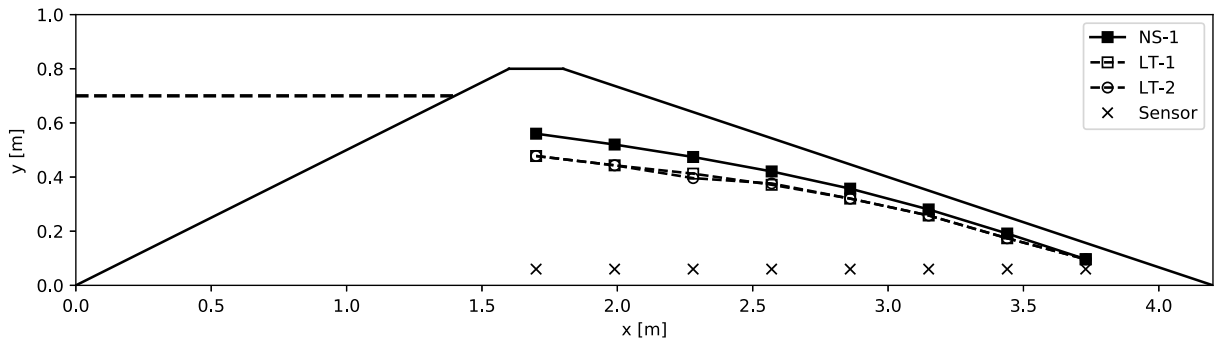

Fig. 13. Reference case numerical and experimental data.

Table 5. Calibration k-factor for NS-1 to fit the results for the reference case, LT-1

	Sensor pair								
	1		3		5		7		
k (m/min)	t_{steady} (min)	Δt (min)	t_{steady} (min)	Δt (min)	t_{steady} (min)	Δt (min)	t_{steady} (min)	Δt (min)	MAE (min)
5.12×10^{-3}	113	+28	113	+18	112	+30	107	+32	28.13
6.12×10^{-3}	99	+14	99	+4	98	+16	94	+19	14.75
7.12×10^{-3}	89	+4	89	−6	89	+7	85	+10	6.63
7.62×10^{-3}	85	0	85	−10	85	+3	81	+6	4.25
8.12×10^{-3}	82	−3	82	−13	81	−1	78	+3	4.50
LT-1	85	—	95	—	82	—	75	—	—

Note: Δt = difference between LT-1 and NS-1.

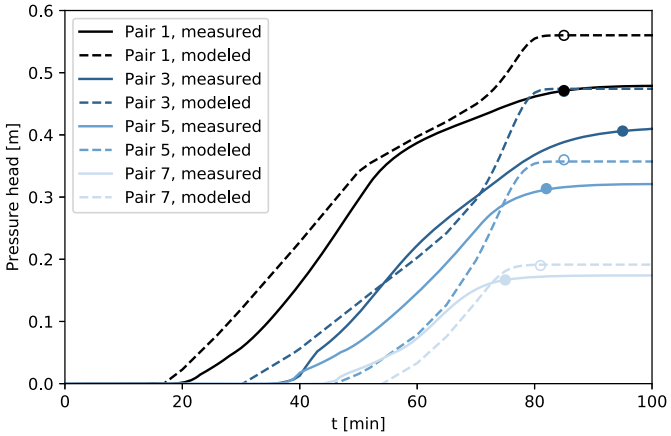

Fig. 14. Pressure head in Sensor pairs 1, 3, 5, and 7 over time for $k = 7.62 \times 10^{-3}$ m/min. LT-1 are the solid lines, NS-1 are dashed lines, and dots indicate steady-state definition.

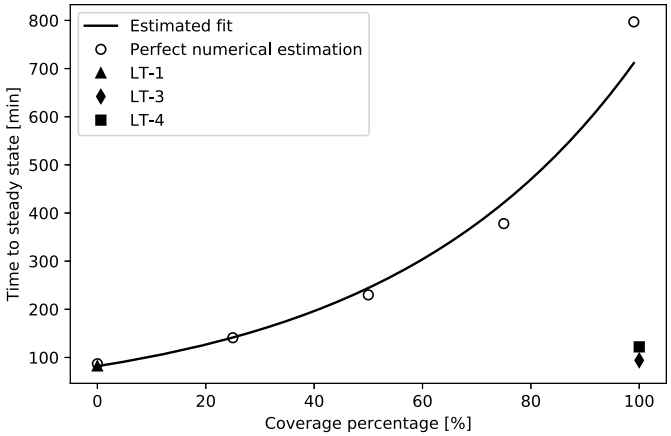

Fig. 15. Time to steady state versus seal-coverage percentages, with exponential fit and measured values.

Table 6. Time to steady state, pressure head in pressure sensor for the various sensor pairs, and steady-state discharge for several outer slope coverage percentages as modeled for ideal seal–surface conditions

Coverage (%)	t_{steady} (min)	h_{steady} (m)				Q_{steady} ($\times 10^{-3}$ L/s)
		Row 1	Row 3	Row 5	Row 7	
0	85	0.56	0.47	0.36	0.19	13.3
25	132	0.52	0.44	0.34	0.19	11.5
50	201	0.47	0.41	0.32	0.19	9.8
−50	85	0.56	0.47	0.36	0.19	13.3
75	378	0.41	0.36	0.29	0.18	8.1
99	797	0.25	0.22	0.18	0.13	4.8

configurations, whereas in the −50% case, the plate covers the lower part. These results indicated that applying a seal on the lower half of the outer slope did not change the pressure at the sensor location when comparing it with the 0% closure case. However, the time to steady state was much longer for the 50% coverage of the upper half of the levee. For the other cases, the steady-state level reduced and the time required to reach these conditions increased.

In Fig. 15, the calculated time to steady state (t_{steady}) is presented for the seal-coverage percentages as presented in Table 6. It was observed that these numerical points closely followed an exponential trend as given by Eq. (2), where C is the numerical value of the seal-coverage percentage. The parameter a was found to be 82 min and b to be 0.02 based on the test data as presented previously. The root mean square error (RMSE) for the given values is 43.4 min, the prediction of the 99% cover value has the largest influence on this error

$$t_{steady} = a \times e^{b \times C} \tag{2}$$

Soil–Seal Interface Layer

To improve the ability of the numerical model to match experimental results, an interface layer was added to the levee surface to take into account the time-delay in reaching steady state, as observed in the data and described in conceptual framework and the previous sections. This allows for a more accurate estimation of the time to steady state when applying a nonperfectly attached seal.

Within the interface layer, two different model parameters are included, the thickness of the interface layer w_g and the permeability of the interface layer k_g (Fig. 2). In the laboratory tests, a distance in the order of 1 cm was observed between the soil and the structure; for that reason, the w_g layer thickness was set to 1 cm. The k_g value will be used as a calibration factor, the calibrated values for the two numerical cases, NS-3 for 99% coverage of plate without toe and NS-4 for 99% coverage of plate with toe, are presented in Table 7. It was found that the interface layer, k_g, led to the best estimation of time to steady state of 2.5 m/min for NS-3 and 1.25 m/min for NS-4.

In Fig. 16, the output of the updated model is compared with the measured values in LT-3 and LT-4 for Sensor pairs 1, 3, 5, and 7. That is now the updated model of the imperfect seal, as described previously, is used. The simulated and obtained time history of the

Table 7. Calibration of k_g for numerical simulations

Simulation	k_g (m/min)	$t_{s,\mathrm{LT,mean}}$ (min)	$t_{s,\mathrm{NS}}$ (min)
NS-3	2.0	94	100
NS-3	2.5	94	94
NS-3	3.0	94	90
NS-4	1.0	122	130
NS-4	1.25	122	118
NS-4	1.5	122	111

Note: LT = results from the laboratory; and NS = results from the numerical simulation.

Table 8. Time to steady-state pressure head for sensor pairs and associated steady-state discharge for the three numerical cases of interest

Test	t_{steady} (min)	h_{steady} (m)				Q_{steady} ($\times 10^{-3}$ L/s)
		Row 1	Row 3	Row 5	Row 7	
NS-1	85	0.56	0.47	0.36	0.19	13.3
NS-3	94	0.55	0.47	0.35	0.19	12.8
NS-4	118	0.52	0.45	0.34	0.19	11.9

pressure head showed reasonably agreement now. The numerically determined time to steady state for NS-3 has become 94 min, and it was 118 min for NS-4. This compares with the experimentally obtained times to steady state of 94 min for LT-3 and 122 min for LT-4.

In NS-3, the steady-state conditions were reached quite abruptly, also when comparing it with NS-1 (Fig. 14) and NS-4 (Fig. 16). This could be explained by the high permeability of the interface layer, which reached steady-state conditions faster than interface layers with a lower permeability. This effect was numerically modeled through the entire levee and deviates from the observed fill curves. The model update found values that were indeed close to the observed ones; thus, the interface layer could be a good representation of imperfect seal–soil conditions.

A summary of the estimated numerical values is shown in Table 8. The reduction in outflow discharge for Numerical cases 1 and 4 is 16.7%, and the measured reduction is 23.5%, which is in the same order of magnitude. The physical measurement did not show a reduction in steady-state pressure height for the first sensor pair (LT-4), whereas the numerical estimates showed a reduction of 8.9%.

Discussion

The results of the research show that a seal has an effect on the spatiotemporal migration of the phreatic surface through a levee. Increasing the time to reach steady-state phreatic conditions will most likely increase the time available until certain failure mechanisms are triggered. These related mechanisms include failure through seepage and slope stability (Schiereck 1998). This extra time allows levee managers extra time to install additional emergency measures or extra time to evacuate people or livestock (Janssen et al. 2021).

Furthermore, the extra time acquired to reach steady-state phreatic conditions should be compared with the duration of a flood wave. This paragraph introduces possibilities to improve the quality of the estimated of the spatiotemporal effects of a seal using numerical models that integrate the interface layer. Furthermore, further research aimed at achieving the optimal effect of a seal is discussed next.

Determine General Parameters Interface Layer

The interface layer added to the numerical simulation was able to capture the reduction of seepage entering the levee taking into account leakage and water flow around a nonperfect seal. In the current analysis on the effect of the interface layer on the spatiotemporal behavior of the phreatic surface level, the k_g and w_g factors were only calibrated for the laboratory case, which consisted of a steel plate. The parameters have not been determined for the field tests within this study. The seal parameters should be determined using a three-dimensional model numerical model to also include the three-dimensional effects of the seal. A two-dimensional model will not be sufficient for the current data set because the seal only had a limited length in the field tests.

The w_g factor of different types of seals should be determined taking the flexibility of the seal into account, together with the irregularities in the outer slope of the levee. The k_g factor has to be calibrated within a numerical model using the data from the field tests. Calibrating the interface layer parameters for different types of seals and varying degrees of levee cover inhomogeneity allows levee managers to estimate the effect of this seal on a levee consisting of

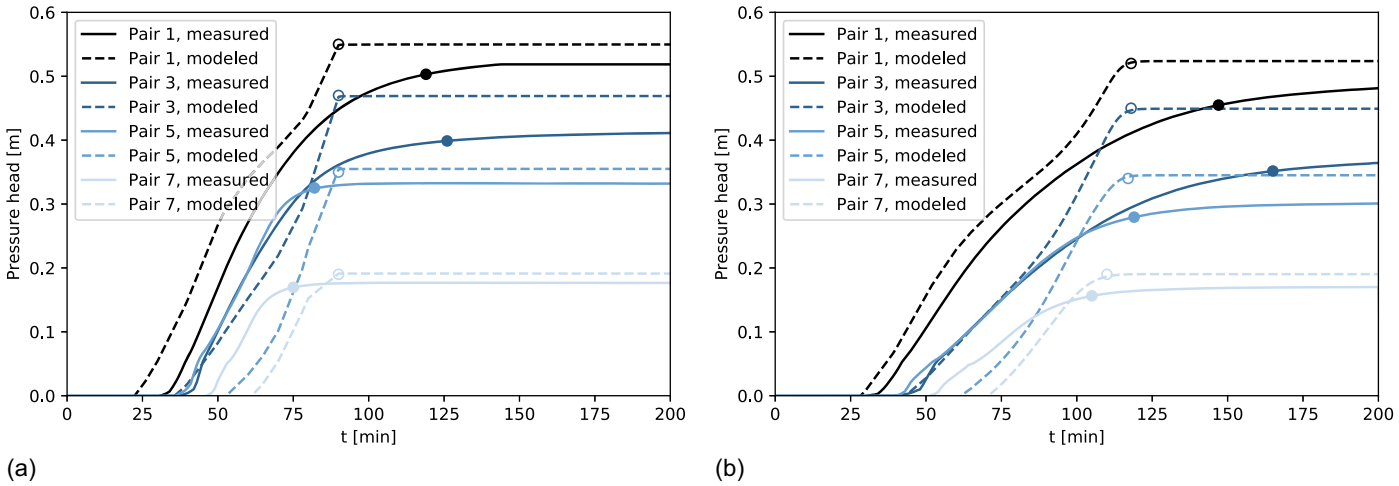

Fig. 16. Measured and simulated data for updated imperfect seal model, both at 99% coverage: (a) Test 3 (LT-3 and NS-3), $k_g = 2.5$ m/min; and (b) Test 4 (LT-4 and NS-4), $k_g = 1.25$ m/min.

local soil materials having a certain geometry. This allows the levee manager to act based on site-specific conditions and provide a corresponding estimate of rise of the phreatic line.

Three-Dimensional Effects of the Seal

The presence a seal seems to have a distinct effect direction alongside the slope (y-direction), illustrated in Fig. 11. This influence area has a certain curvature, which could be identified as bowl-shaped. In the conducted experiments, the width of the seal in y-direction was kept constant. Increasing the width of the seal will increase the spatial-temporal area affected by the phreatic surface. Further research should be conducted to determine the minimal required seal dimensions to acquire a local increment in levee stability over a certain amount of distance. This knowledge helps emergency response managers to determine the minimal required length of seal to optimize its effect on flood risk safety.

Conclusions

Here, we studied the effect of a seal on the development of the phreatic level in space and time in a levee during a high-water event. Increasing phreatic water levels will negatively affect the safety and integrity of the levee, particularly for internal erosion and instability. We presented a conceptual framework, laboratory experiments, field experiments, and numerical simulations for configurations of increasing complexity. This provided insight into the response of the phreatic level following a sudden rise of riverside water levels for a case in which a seal has been placed on the outer slope of the levee.

Three different laboratory experiments have been conducted within the research on a heterogeneous sand levee: a reference case, a case where the outer slope was covered by an impermeable seal plate, and a case with a steel plate where the inflow of sand was obstructed by a sandy toe. For all of the experiments, the steady-state phreatic level was approximately the same. However, an increase in time to reach steady state was observed of 25% for the sealed case and 50% for the sealed case with a toe. The largest effect of the seal was mainly in the early phase of the experiments.

In the field tests, the three-dimensional effects of a seal on a heterogeneous levee have been explored. The tests consisted of a reference case, a case covered with a plywood plate, and a case with a flexible seal. All of the mentioned tests were conducted with and without damage to the outer slope of the levee. The field tests showed a negligible beneficial effect on the steady-state phreatic level by an impermeable plate. In the case where the seal was applied on a levee without damage to the outer slope, the time to reach steady state increased by 12% compared with the reference case. For a levee with a damaged slope and more potential infiltration, an impermeable seal increased the time to reach steady-state conditions by 20%.

The time-delay effect of a seal on the phreatic surface for three-dimensional, heterogeneous field trials, and two-dimensional homogeneous laboratory tests were consistent. A seal that can adjust itself to the outer slope, i.e., a flexible layer that folds over surface irregularities on the levee slope, led to an increase of the time to reach the steady-state conditions in the levee volume directly underneath the seal. Idealized numerical conditions showed that a seal can increase the time required to reach steady-state conditions by a factor of 2.5 when covering half of the outer slope.

To properly model the influence of a seal on the spatiotemporal development of the phreatic line, an interface layer was introduced, consisting of a certain width and hydraulic conductivity. The width of the interface layer in the model is the maximum observed distance between the seal and the surface. The hydraulic conductivity of the interface layer is a calibration parameter that represents the percentage of slope covered by the seal. Numerical model runs of the laboratory case showed that the presented interface layer can be used to quite accurately match the experiments.

The delays found in reaching steady-state conditions can contribute to postponing or preventing levee failure triggered by either slope instabilities or internal erosion. For that reason, sealing of the outer slope of a levee is only recommended as a preventive measure, which should be applied before the phreatic surface of the levee reaches the steady-state conditions. For practical reasons, the seal should be placed before the water level rises when installing it from the land. However, when using waterborne emergency measures, one could extend the time frame for placement.

Future research should improve the predictability of the sealing effect, allowing practitioners to use simple calculations to estimate the extra time acquired and the quantity of seal required to achieve this effect. Eq. (2) gives a reasonable prediction of the expected time to steady state with a coverage percentage in ideal conditions, but for more precise predictions, more elaborate models are recommended. Also, the results of this study can be used to develop and improve emergency procedures for flood fighting using measures for sealing (parts of) flood defenses.

Data Availability Statement

The data that support the findings of this study are openly available in 4TU.ResearchData at https://doi.org/10.4121/152663fc-0e02-46bf-a0c7-2ebb7b509f68 (Janssen 2023).

Acknowledgments

The research was funded by the Dutch Ministry of Defense. Measurement devices in Flood Proof Holland are funded by the Interreg Polder 2C's project. The authors want to thank the technicians of the TU Delft Hydraulic Engineering Laboratory and the Netherlands Defence Academy. Furthermore, special gratitude for VP Delta for providing access to their test facility Flood Proof Holland. At last, all students involved in the experimental modeling are acknowledged for their contribution.

Notation

The following symbols are used in this paper:

C = percentage of plate covering the outer levee slope (%);
c = cohesion (kPa);
h = pressure head (m);
h_{steady} = steady-state pressure head (m);
i = gradient of the flow;
i_{cr} = critical gradient of the flow;
k = hydraulic conductivity (m/min);
k_g = hydraulic conductivity interface layer (m/min);
L_p = effective length covered by seal, from water level to bottom seal (m);
L_w = effective length not covered by seal, from toe of levee to bottom seal (m);
p = pore water pressure (kPa);
Q_{steady} = steady-state discharge through levee (L/s);
q = Darcy velocity (m/s);
S_s = degree of saturation;

t = time (min);
t_{steady} = time required to reach steady-state conditions (min);
w_g = thickness interface layer between seal and levee (m);
γ = specific weight soil (kN/m^3);
γ_w = specific weight water (kN/m^3);
Δh = difference in steady-state pressure head (m);
Δt = time difference to reach steady-state conditions (min);
σ = total soil stress (kPa);
σ' = effective soil stress (kPa); and
φ = angle of internal friction (degrees).

References

Beber, R., A. Tarantino, and P. Becker. 2023. "Climate change adaptation of Elbe river flood embankments via suction-based design" *Int. J. Geomech.* 23 (3): 05023001. https://doi.org/10.1061/IJGNAI.GMENG-7693.

Bentley Systems Team. 2021. "PLAXIS LE 1D/2D/3D saturated/unsaturated finite element groundwater modeling (theory manual)." Accessed March 17, 2023. https://communities.bentley.com/products/geotech-analysis/w/wiki/52921/manuals---plaxis-le.

CIRIA (Construction Industry Research and Information Association). 2013. *The international levee handbook*. London: CIRIA.

Fredlund, D. G., and A. Xing. 1994. "Equations for the soil-water characteristic curve." *Can. Geotech. J.* 31 (4): 521–532. https://doi.org/10.1139/t94-061.

Hofmann, M., M. Grimmer, and J. Steuernagel. 2006. *Instruktion zur Deichverteidigung*. Darmstadt, Germany: Regierungspräsidium Darmstadt.

Hommes, D. P. 2022. "BresDefender: The effect of an emergency measure on the phreatic surface of a dike in space and time." M.Sc. thesis, Dept. of Hydraulic Structures and Flood Risk, TU Delft.

Janssen, D. 2023. "Dataset: BresDefender, An experimental study on an emergency response measure for levee breaches." Accessed December 1, 2023. https://doi.org/10.4121/152663fc-0e02-46bf-a0c7-2ebb7b509f68.v1.

Janssen, D., A. J. M. Schmets, B. Hofland, E. Dado, and S. N. Jonkman. 2021. "BresDefender: A potential emergency measure to prevent or postpone a dike breach." In *Proc., FLOODrisk2020: 4th European Conf. on Flood Risk Management*. Les Ulis, France: EDP Sciences. https://doi.org/10.3311/FloodRisk2020.19.3.

Rahimi, A., H. Rahardjo, and E.-C. Leong. 2015. "Effects of soil–water characteristic curve and relative permeability equations on estimation of unsaturated permeability function." *Soils Found.* 55 (6): 1400–1411. https://doi.org/10.1016/j.sandf.2015.10.006.

Rijkswaterstaat. 2019. "Schematiseringshandleiding microstabiliteit." Accessed November 10, 2023. www.helpdeskwater.nl.

Schiereck, G. 1998. "Grondslagen voor waterkeren. report, Rijkswaterstaat, 1998b." Accessed April 14, 2022. https://resolver.tudelft.nl/uuid:3bcbbc42-b1a4-4796-80ef-90dd3acf1198.

Schindler, U. 1980. "Ein Schnellverfahren zur Messung der Wasserleitfähigkeit im teilgesättigten Boden an Stechzylinderproben." *Archiv für Acker- und Pflanzen-bau und Bodenkunde* 4 (1): 1–7.

TAW (Technische Adviescommissie Voor de Waterkeringen). 1995. *Druk op de dijken 1995: De toestand van de rivierdijken tijdens het hoogwater van januari-februari 1995*. Delft, Netherlands: TAW Publicatie.

Vahedifard, F., F. H. Jasim, F. T. Tracy, M. Abdollahi, A. Alborzi, and A. AghaKouchak. 2020. "Levee fragility behavior under projected future flooding in a warming climate." *J. Geotech. Geoenviron. Eng.* 146 (12): 04020139. https://doi.org/10.1061/(ASCE)GT.1943-5606.0002399.

Van, M. A., E. Rosenbrand, R. Tourment, P. Smith, and C. Zwanenburg. 2022. "Failure paths for levees." In *Proc., Int. Society of Soil mechanics and Geotechnical Engineering (ISSMGE), Technical Committee TC201 'Geotechnical Aspects of Dikes and Levees'*. London: International Society of Soil mechanics and Geotechnical Engineering. https://doi.org/10.53243/R0006.

Van Den Berg, F. P. W., and A. R. Koelewijn. 2023. "Graverij door dieren, Verschillende praktijkcases, inspectietechnieken en uitsplitsing invloed op overstromingskans." Accessed January 13, 2024. https://publications.deltares.nl/11209262_001_0001.pdf.

Žilys, V., N. Jakštienė, M. Jasiulionis, and A. Ulevičius. 2009. "Morphological alteration of land reclamation canals by beavers (*Castor fiber*) in Lithuania." *Estonian J. Ecol.* 58 (2): 126–140. https://doi.org/10.3176/eco.2009.2.06.